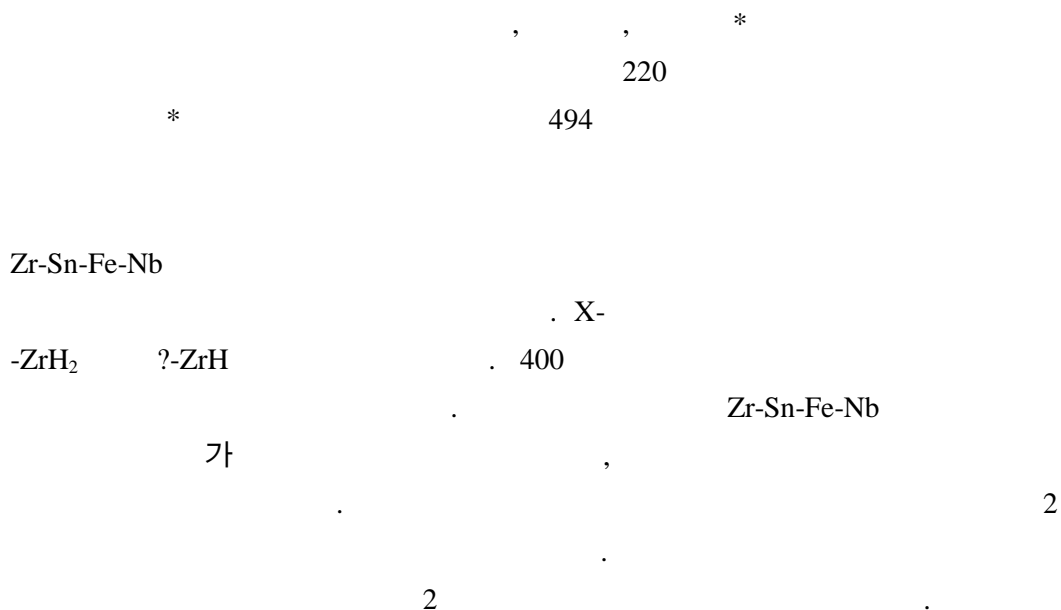


2002

Zr-Sn-Fe-Nb

Effect of Zirconium Hydrides on the Deformation Behavior of Zr-Sn-Fe-Nb Tubes



Abstract

The characteristics of zirconium hydrides formed by a electrochemical hydrogen charging method and their effect on the mechanical properties of Zr-Sn-Fe-Nb tubes were investigated. The hydrides were observed to be mostly circumferentially oriented and were identified as ϵ -ZrH₂ and γ -ZrH phases by X-ray diffraction. The distribution of hydrides was found to become more homogeneous when the cooling rate is higher from 400°C. The room temperature strength of Zr-Sn-Fe-Nb tubes increased slightly and the ductility decreased with the formation of the hydrides. The mechanical properties were slightly modified by the size and distribution of hydrides. Secondary cracks along the platelets of hydrides were observed on the fracture surfaces of tubes. The slight loss of ductility in the presence of circumferential hydrides is thought to be associated with the secondary cracking during the final process of the fracture.

가 (1- 가 8) 가

(9)

(10)

가

가

(10,14)

Nb

가

Zr-Sn-Fe-
Zr-Sn-Fe-Nb

Zr-Sn-Fe-Nb

Zr-Sn-Fe-Nb

30°

Zircaloy-4

(6)

9.5mm 8.4mm , . 1

(8)

0.2 0.5A/cm2

Zircaloy

(11)

working electrode counter electrode

record

working electrode reference electrode

attached burette

가

1260ppm⁽⁸⁾

400

3

4 /sec

126 /sec

X-ray diffractometer(Ziemens)

ring

가

4.5mm

grip

1 ring

ring

1mm

United Testing Machine(SFP 10)

5mm

Ref.6.

JEOL-6400

2 Zr-Sn-Fe-Nb 400 3

(8), (a) (b)

3 Zr-Sn-Fe-Nb X-peak가

face centered tetragonal (ZrH) (ZrH₂)가 (ZrH) c/a 가 1 (ZrH₂) c/a 가 1¹²⁾

4 () Zr-Sn-Fe-Nb 가

Zr-Sn-Fe-Nb¹²⁾

5 Zr-Sn-Fe-Nb

(a) (b) (c)

Zr-Sn-Fe-Nb(b) 2 20 30μm 2

6 (a) (b)

6(b) 2 Zr-Sn-Fe-Nb

13)

$$V_{app} = kT \frac{\partial \ln \dot{\mathbf{g}}}{\partial t} \cong kT \frac{\ln(\dot{\mathbf{e}}_1 / \dot{\mathbf{e}}_2)}{\mathbf{t}_1 - \mathbf{t}_2} \quad (1)$$

k Boltzmann, r, τ₁, τ₂, ?₁

?₂, T, τ, σ_y Taylor m

, τ = σ_y/m, Luton Jonas HCP m 4

4) Zr-Sn-Fe-Nb

46b³(b Burgers vector), Zr-Sn-Fe-Nb 41b³

0.03,

1.17 × 10⁻² 1.34 × 10⁻² 가 Zr-Sn-Fe-Nb¹⁴⁾

Zircaloy-4

가

5

10 μ m

, Zircaloy-4

Al

10-20 μ m

가

Hong

(15,16)

. Zr-Sn-Fe-Nb

. Zr-Sn-Fe-Nb

Zircaloy-4

(14-17)

, Zr-Sn-Fe-Nb

Zircaloy-4

. Hong

(17)

Zircaloy-4

2

가

Zr-Sn-Fe-Nb

1.

Zr-Sn-Fe-Nb

, X-

?-ZrH

-ZrH₂

2.

3.

2

4.

Reference

1. B. Cox and Y. M. Wong, *J. Nucl. Mater.*, 270 (1999) 134.
2. J. B. Bai, N. Ji, D. Gilbon, C. Prioul and D. Francois, *Metall. Mater. Trans.*, 25A (1994) 1199.
3. S. I. Hong, W. S. Ryu and C. S. Rim, *J. Nucl. Mater.*, 120 (1984) 1.
4. S. I. Hong, W. S. Ryu and C. S. Rim, *J. Nucl. Mater.*, 116 (1983) 314.
5. J. L. Derep, S. Ibrahim, R. Rouby and G. Fantozzi, *Acta Metall.*, 28 (1980) 607.
6. K. W. Lee, S. K. Kim, K. T. Kim and S. I. Hong, *J. Nucl. Mater.*, 295 (2001) 21.
7. B. A. Cheaddle, *Physical Metallurgy of Zirconium Alloys*, CRNL Report, CRNL-1208 (1974).
8. Y. Choi, J. W. Lee, Y. W. Lee and S. I. Hong, *J. Nucl. Mater.*, 256 (1998) 124.
9. F. Garzarolli, R. V. Jan, H. Stehle, *Atomic Energy Rev.*, 17 (1979) 31.
10. L. G. Bell and R. G. Duncan, *AECL Report*, AECL-5110 (1975).
11. A Sawatzky, *J. Nucl. Mater.*, 2 (1962) 62.
12. D. O. Northwood and U. Kosasih, *Int'l Metals reviews*, 28 (1983) 92.
13. H. Conrad, *J. Met.*, 16 (1964) 582.
14. J. S. Song, S. D. Kim, S. I. Hong, Y. Choi and J. W. Kim, *J. Korean Inst. Metall. Mater.*, 35 (1997) 1668.
15. S. I. Hong, G. T. Gray III and J. J. Lewandowski, *Acta Metall. Mater.*, 41 (1993) 2337.
16. S. I. Hong and G. T. Gray III, *J. Mater. Sci.*, 29 (1994) 2987.
17. S. I. Hong, K. W. Lee and K. T. Kim, *J. Nucl. Mater.*, accepted 22 February (2002).

Table 1. Chemical composition of zirconium alloy tube used in this study.

Sn	Fe	Nb	O	Zr
0.7	0.74	0.74	0.13	Bal.

Figure Captions

Fig. 1. Schematic configuration of tensile testing sample and grip.

Fig. 2. Three-dimensional view of Zr-Sn-Fe-Nb tube with hydrides. Air cooled (a) and furnace-cooled (b).

Fig. 3. X-ray diffraction spectra obtained from hydrided Zr-Sn-Fe-Nb tube

Fig. 4. Stress-strain responses of non-hydrided and hydrided Zr-Sn-Fe-Nb tubes.

Fig. 5. Fracture surfaces of as-received (a) and hydrided (b) Zr-Sn-Fe-Nb tubes. Air cooled (b) and furnace cooled (c) tubes.

Fig. 6. Transverse sections of the air-cooled (a) and furnace-cooled (b) Zr-Sn-Fe-Nb tubes after fracture.

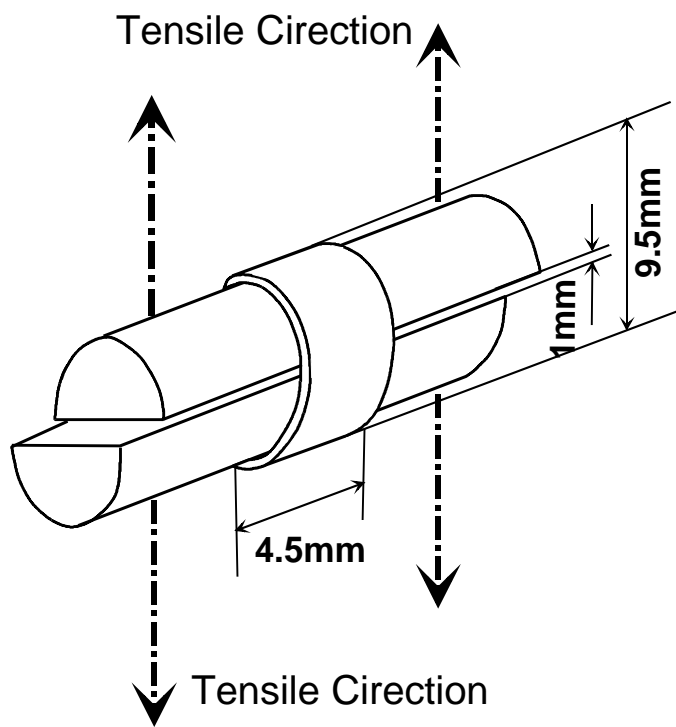


Fig. 1. Schematic configuration of tensile testing sample and grip.

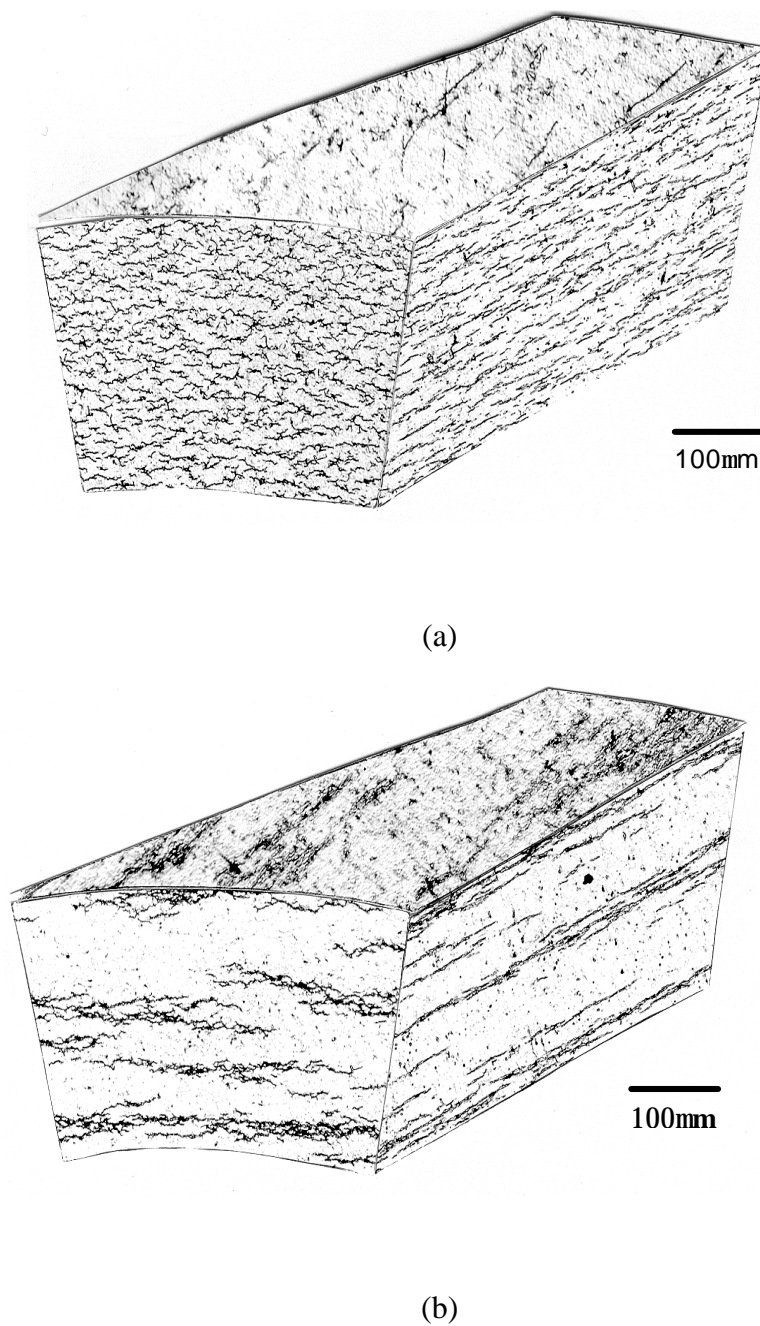


Fig. 2. Three-dimensional view of Zr-Sn-Fe-Nb tube with hydrides. Air cooled (a) and furnace-cooled (b).

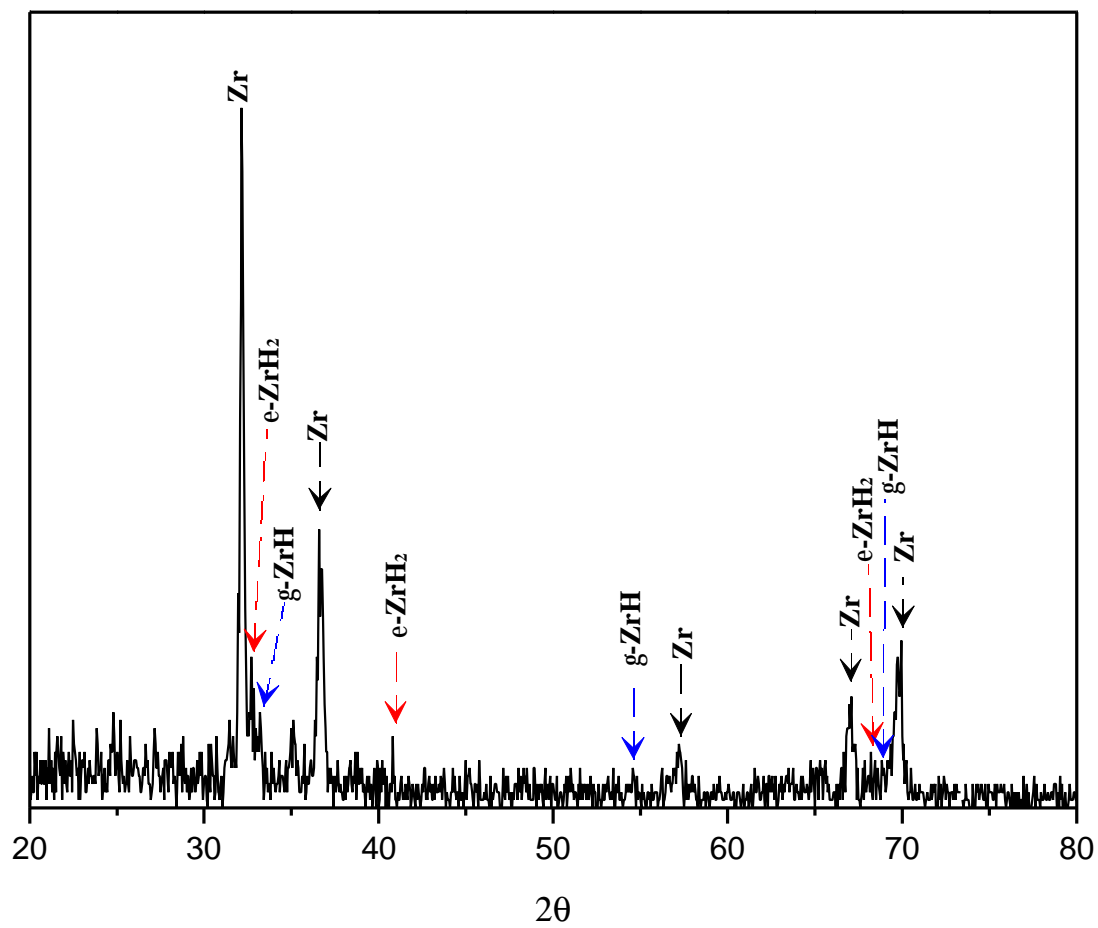


Fig. 3. X-ray diffraction spectra obtained from hydrided Zr-Sn-Fe-Nb tube

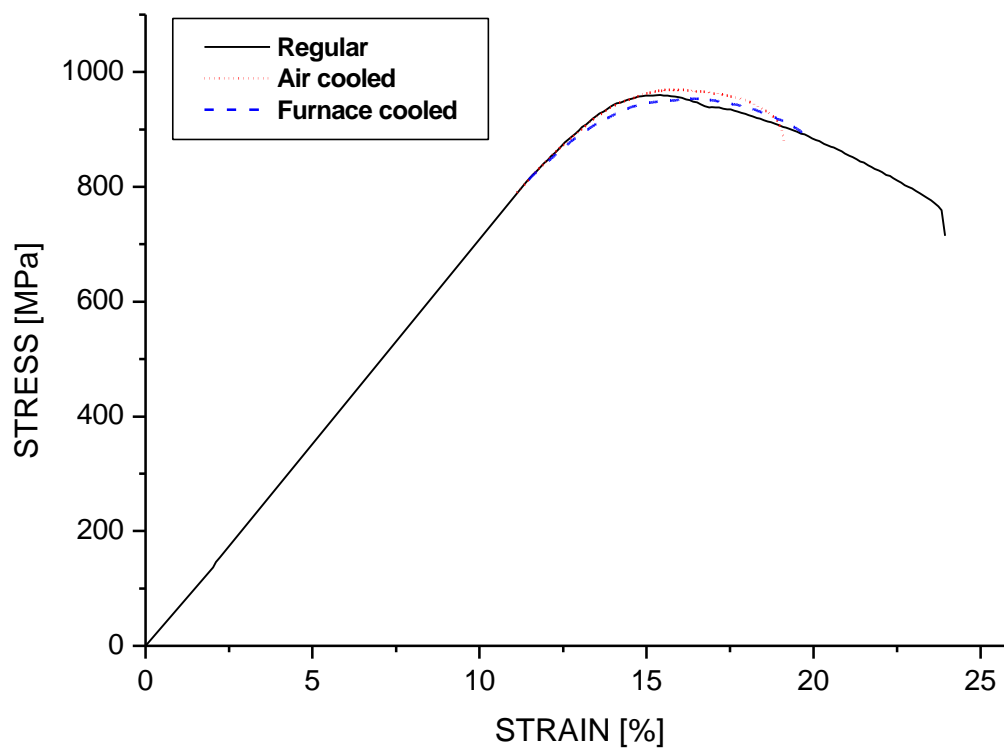
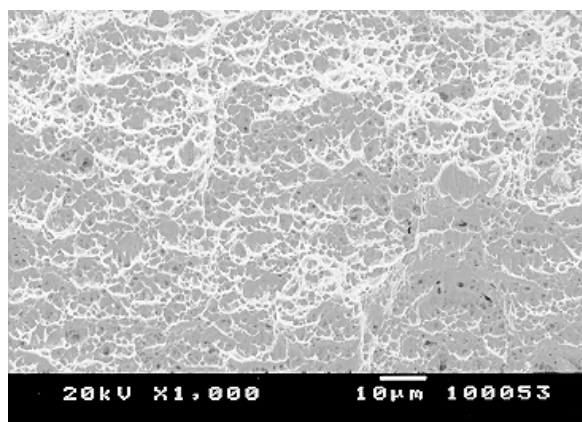
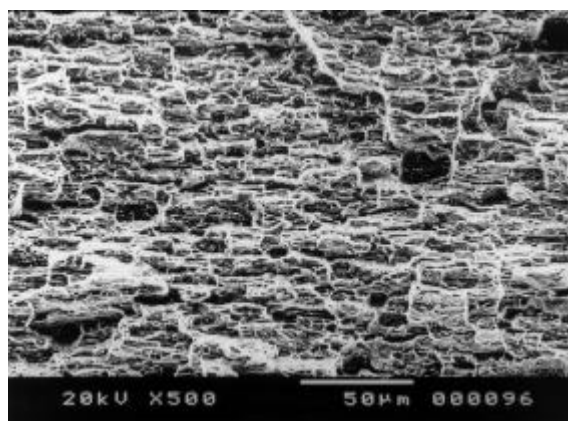


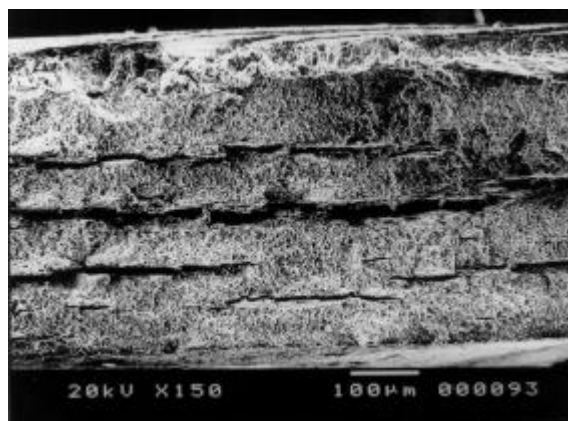
Fig. 4. Stress-strain responses of non-hydrated and hydrated Zr-Sn-Fe-Nb tubes



(a)

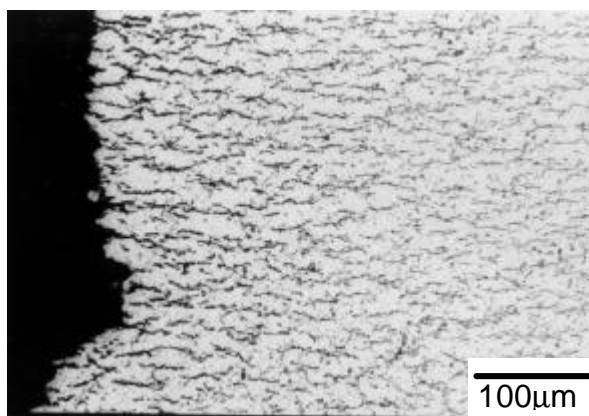


(b)

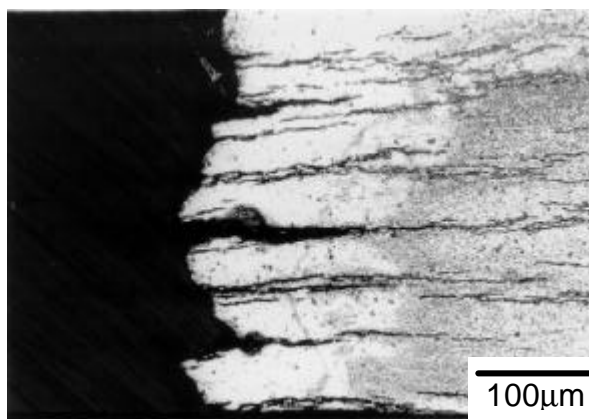


(c)

Fig. 5. Fracture surfaces of as-received (a) and hydrided (b) Zr-Sn-Fe-Nb tubes. Air cooled (b) and furnace cooled (c) tubes



(a)



(b)

Fig. 6. Transverse sections of the air-cooled (a) and furnace-cooled (b) Zr-Sn-Fe-Nb tubes after fracture